Title
Inhibition of Epithelial-to-Mesenchymal Transition and Pulmonary Fibrosis by Methacycline

Journal
American Journal of Respiratory Cell and Molecular Biology, 50(1)

ISSN
1044-1549

Authors
Xi, Ying
Tan, Kevin
Brumwell, Alexis N
et al.

Publication Date
2014

DOI
10.1165/rcmb.2013-0099oc

Peer reviewed

ORIGINAL RESEARCH

Inhibition of Epithelial-to-Mesenchymal Transition and Pulmonary Fibrosis by Methacycline

Ying Xi[1], Kevin Tan[1], Alexis N. Brumwell[1], Steven C. Chen[2], Yong-Hyun Kim[1], Thomas J. Kim[1], Ying Wei[1], and Harold A. Chapman[1]

[1]Pulmonary and Critical Care Division and Department of Medicine, and [2]Department of Pharmaceutical Chemistry and Small Molecule Discovery Center, University of California San Francisco, San Francisco, California

Abstract

A high-throughput small-molecule screen was conducted to identify inhibitors of epithelial–mesenchymal transition (EMT) that could be used as tool compounds to test the importance of EMT signaling *in vivo* during fibrogenesis. Transforming growth factor (TGF)-β1–induced fibronectin expression and E-cadherin repression in A549 cells were used as 48-hour endpoints in a cell-based imaging screen. Compounds that directly blocked Smad2/3 phosphorylation were excluded. From 2,100 bioactive compounds, methacycline was identified as an inhibitor of A549 EMT with the half maximal inhibitory concentration (IC50) of roughly 5 μM. *In vitro*, methacycline inhibited TGF-β1–induced α-smooth muscle actin, Snail1, and collagen I of primary alveolar epithelial cells . Methacycline inhibited TGF-β1–induced non-Smad pathways, including c-Jun N-terminal kinase, p38, and Akt activation, but not Smad or β-catenin transcriptional activity. Methacycline had no effect on baseline c-Jun N-terminal kinase, p38, or Akt activities or lung fibroblast responses to TGF-β1. *In vivo*, 100 mg/kg intraperitoneal methacycline delivered daily beginning 10 days after intratracheal bleomycin improved survival at Day 17 ($P < 0.01$). Bleomycin-induced canonical EMT markers, Snail1, Twist1, collagen I, as well as fibronectin protein and mRNA, were attenuated by methacycline (Day 17). Methacycline did not attenuate inflammatory cell accumulation or alter TGF-β1–responsive genes in alveolar macrophages. These studies identify a novel inhibitor of EMT as a potent suppressor of fibrogenesis, further supporting the concept that EMT signaling is important to lung fibrosis. The findings also provide support for testing the impact of methacycline or doxycycline, an active analog, on progression of human pulmonary fibrosis.

Keywords: Jun kinase; signaling; Snail1; tetracycline

Clinical Relevance

The findings of this study indicate that there are derivatives of tetracycline active in inhibition of fibrogenesis in a preclinical model. Therefore, independent of any antibiotic activity, such derivatives may have therapeutic activity in fibrotic diseases.

Several lines of evidence indicate that altered distal airway/alveolar epithelial cell signaling is intricately involved in the initiation and progression of pulmonary fibrosis. Genetic mutations in surfactant proteins made exclusively by type II alveolar cells result in fibrotic forms of interstitial lung disease (1). Studies of endoplasmic reticulum stress indicate epithelial cells display signs of such stress in both histologically uninjured and injured regions of lungs of patients with idiopathic pulmonary fibrosis (IPF) (2–4). Experimentally, epithelial endoplasmic reticulum stress potentiates other fibrogenic agents to promote fibrosis (5, 6). One implication of this body of work is that stress-induced epithelial cell signaling must in some way communicate with mesenchymal cells to propagate an exaggerated repair, leading to excessive fibrosis (7). Prior studies have elucidated several signaling pathways connecting stimulated epithelial cells with mesenchymal cell expansion (8, 9). These include loss of epithelial release of prostaglandin E2, a suppressor of fibroblast

(Received in original form March 4, 2013; accepted in final form July 12, 2013)

This work was supported by National Institutes of Health grants HL44712 and HL108794, and a University of California San Francisco biomedical research award through the Sandler Program in Basic Sciences.

Correspondence and requests for reprints should be addressed to Harold A. Chapman, M.D., Pulmonary and Critical Care Division, University of California at San Francisco, 513 Parnassus Avenue, San Francisco, CA 94143-0130. E-mail: hal.chapman@ucsf.edu

This article has an online supplement, which is accessible from this issue's table of contents at www.atsjournals.org

Am J Respir Cell Mol Biol Vol 50, Iss 1, pp 51–60, Jan 2014

Originally Published in Press as DOI: 10.1165/rcmb.2013-0099OC on August 14, 2013
Internet address: www.atsjournals.org

activation, as well as heightened expression of connective tissue growth factor and transforming growth factor (TGF)-β1 (10–12). Epithelial-specific activation of latent TGF-β1 appears critical to lung fibrogenesis (13). Active TGF-β1 may act in a paracrine manner with nearby resident fibroblasts to promote their proliferation and collagen deposition. Epithelial cells also respond directly to TGF-β1 by developing an epithelial-to-mesenchymal transition (EMT) (14, 15). EMT signaling potentially leads to both activation of collagen and other genes encoding mesenchymal proteins, as well as altered signaling, such as up-regulation of connective tissue growth factor and TGF-β1 itself, which potentiates the repair process.

The degree to which alveolar epithelial cells acquire mesenchymal features during fibrotic processes in the lung and the importance of EMT signaling to lung fibrogenesis remains uncertain (16). Recent evidence linking signaling pathways promoting EMT *in vitro* with fibrogenesis *in vivo* supports an important role for EMT signaling in fibrosis (5, 6, 17–22). Moreover, epithelial-specific expression of the canonical EMT transcription factor, Snail1, is required for experimental hepatic fibrosis (23). To further explore this issue in the lung, we undertook an unbiased screen of bioactive compounds that inhibit EMT in human lung epithelial cells to develop tools that could be used *in vivo* to test whether EMT is relevant to lung fibrogenesis. An important feature of this screen is that only compounds that blocked EMT, but did not directly affect TGF-β1 receptor kinase activity, were studied further. This report is focused on one of the compounds that emerged from this screen, the antibiotic and tetracycline family member, methacycline.

Materials and Methods

See the online supplement for additional details.

High-Throughput Screen

A549 cells were cultured on tissue culture cyclo-olefin polymer in black Aurora 384-well plates (Brooks Automation, Poway, CA) at the density of 1,500 cells per well, and, on the second day, cells were washed three times with PBS. Compounds/cytokines were then added via a Beckman Coulter Biomek FXp liquid handling workstation (Beckman Coulter, Brea, CA) in serum-free medium. After 48 hours, cells were washed and stained for E-cadherin (Alexa488), fibronectin (Alexa568), and 4′,6-diamidino-2-phenylindole via a Bio-Tek EL406 microplate washer/dispenser (BioTek, Winooski, VT), and then imaged in a GE IN Cell 2,000 automated fluorescent microscope (GE Healthcare Life Sciences, Pittsburgh, PA). Next, the IN Cell Developer (GE Healthcare Life Sciences) was used to quantify images, and was capable of reporting multiple aspects of the image, including size and intensity of the cell nuclei, cytoplasm, and membrane. The Z prime for this methodology, comparing untreated and TGF-β1–treated cells, is roughly 0.5 (calculated online at https://smdc.ucsf.edu/). Detailed imaging and analysis information is provided in the online supplement.

Bleomycin Fibrosis Model

Female C57BL/6 mice (6–8 wk old) were intratracheally instilled with saline or 2.0–2.5 U/kg of bleomycin (Sigma-Aldrich, St. Louis, MO). Cohorts of mice were injected intraperitoneally with methacycline (100 mg/kg/d) dissolved in saline daily beginning on Day 10 after bleomycin. Control animals received vehicle alone in the same formulation. Mice were killed on Day 17. The lungs were lavaged, followed by optimal cutting temperature compound embedding for imaging or snap freezing in liquid nitrogen for protein extraction.

Measurements of Lung Collagen

Total lung collagen levels were determined by measuring acid and pepsin-soluble collagen in both lungs using a Sircol collagen assay kit (Biocolor Ltd, Carrickfergus, County Antrim, UK) according to the manufacturer's instructions. For histological assessment of lung collagen, frozen sections of the left lung were stained using Masson's trichrome stain kit (American MasterTech, Lodi, CA). The whole section was imaged with a Zeiss Axio upright microscope and tiled using 10% image overlap into a single panoramic by Axiovision 4.7 software (Zeiss, Jena, Germany). The area and intensity of trichrome staining was then quantified using NIH ImageJ software (Natioanl Institutes of Health, Bethesda, MD). To further define collagen I protein and mRNA levels, snap-frozen lungs were ground into tissue powder before lysis. The tissue powder was either lysed in RIPA buffer for blotting or lysed in Trizol reagent (Invitrogen, Grand Island, NY) for RNA isolation and quantitative PCR analysis. Bronchoalveolar lavage (BAL) collagen I was measured by blotting of 50 μl supernatant from 1 ml BAL.

Reporter Activity Assay

T cell factor (TCF) reporter plasmid (TOPFlash) (EMD Millipore, Billerica, MA), TCF reporter plasmid with mutated TCF bindng sites (FOPFlash) (EMD Millipore), or 12× Smad-binding element (SBE) plasmid (Addgene, Cambridge, MA) was cotransfected in A549 cells with *Renilla* luciferase pRL-TK Reporter (Promega, Madison, WI) using lipofectamine 2,000 reagent (Invitrogen) according to the manufacturer's protocol. At 48 hours after transfection, cells serum starved overnight were stimulated with TGF-β1 (4 ng/ml) for 24 hours in serum-free medium, and reporter activity was determined using a dual luciferase reporter system (Promega), according to the manufacturer's instructions.

Statistics

Variance for all group data is expressed as SEM. For evaluation of group differences, the unpaired two-tailed Student's *t* test was used assuming equal variance. A P value less than 0.05 was accepted as significant.

Results

Identification of Methacycline as a Lead Compound for Blockade of EMT in A549 Cells and Primary Lung Epithelial Cells

A 2,100-compound library, which includes 60% known drugs, 25% natural products, and 15% other bioactive components (Microsource [http://www.msdiscovery.com/spectrum.html]) was screened for small-molecule inhibitors of EMT at the University of California at San Francisco Small Molecule Discovery Center (http://smdc.ucsf.edu). The screen was based on 48-hour culture of A549 cells with and without TGF-β1, and then imaging for up-regulation of fibronectin (*red*) and down-regulation of E-cadherin (*green*; Figure 1A). Quantitative pixel data were normalized as percentage intensity relative to a positive control SB431542, a direct

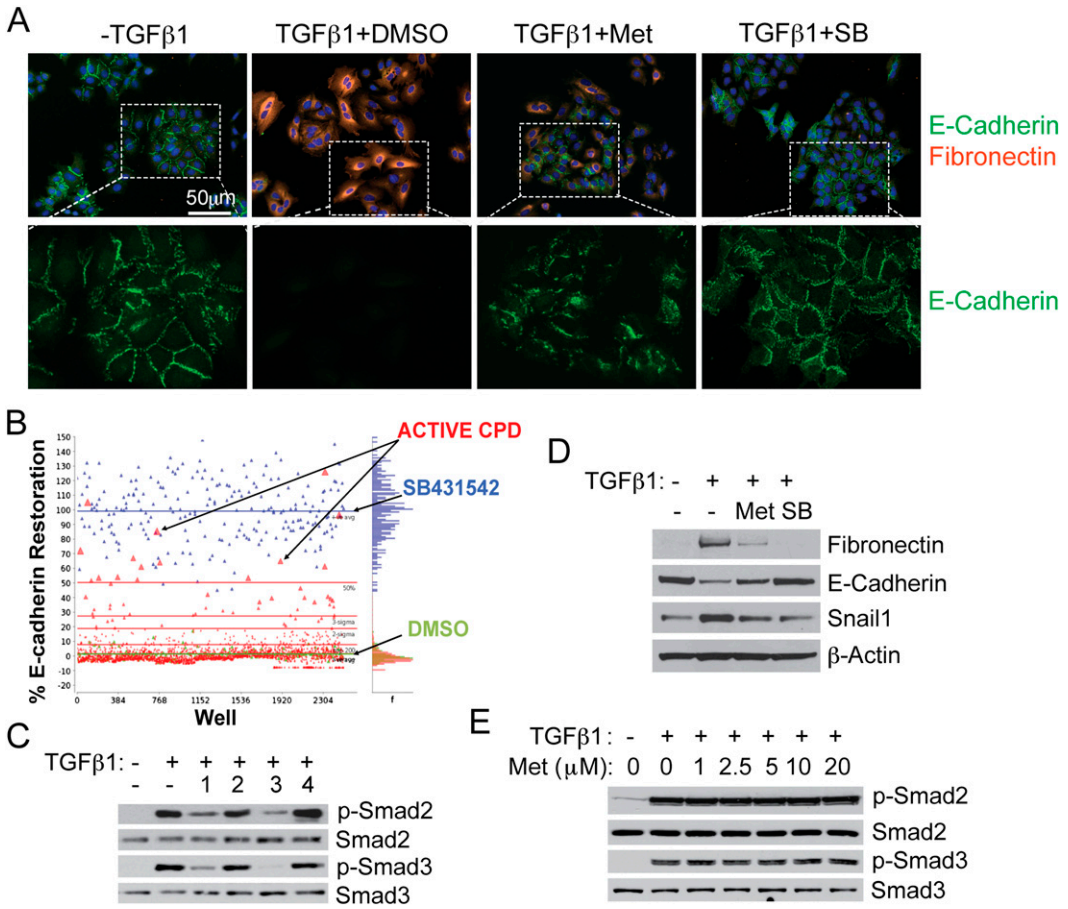

Figure 1. High-throughput screen of small-molecule library for epithelial–mesenchymal transition (EMT) inhibitors. (*A*) Immunofluorescence imaging of A549 cells with and without transforming growth factor (TGF)-β1 (4 ng/ml) for 48 hours in the presence of dimethyl sulfoxide (DMSO), methacycline (Met; 10 μM), or SB431542 (SB; 5 μM). E-cadherin, *green*; fibronectin, *red*. *Scale bar*, 50 μm. (*B*) Scatter plot showing primary screen of EMT inhibitors. Vehicle controls (DMSO only), *green*; test compounds in DMSO, *red*; SB in DMSO, *blue*. *Triangles* indicate active compounds (ACTIVE CPD) that inhibit over 50% of E-cadherin loss. (*C*) A549 cells serum starved overnight were stimulated with TGF-β1 (4 ng/ml) in the presence of compound 1, 2, 3, and 4 (Met; 10 μM) for 1.5 hours and the lysates were blotted for phosphorylated Smad (p-Smad) -2, and p-Smad3, total Smad2, and Smad3 are used as loading control. (*D*) A549 cells stimulated with TGF-β1 (4 ng/ml) were treated with Met (10 μM) or SB (5 μM) for 48 hours and the lysates were blotted for fibronectin, E-cadherin, and Snail1. β-actin is used as loading control. (*E*) A549 cells serum starved overnight were stimulated with TGF-β1 (4 ng/ml) in the presence of Met (0–20 μM) for 1.5 hours and the lysates were blotted for p-Smad2 and p-Smad3. Total Smad2 and Smad3 are used as loading control. (*D–E*) A representative blot of three independent experiments is shown.

inhibitor of TGF-β1 receptor kinase (ALK5).

As displayed in Figure 1B, in *red* are test compounds (added in dimethyl sulfoxide at 5 μM final concentration) and in *blue* are the effects of positive control SB431542, added in multiple wells to each test plate. The figure shows percent inhibition of E-cadherin loss. Only compounds that restored E-cadherin more than 50% after TGF-β1 stimulation and suppressed fibronectin more than 50% in the parallel fibronectin induction imaging were tested further. Based on these criteria, 16 compounds were identified, but, after scrutiny of the images for healthy epithelial morphology, only four compounds were judged to be candidate inhibitors for further testing (a manageable approximately 0.2% hit rate). The four compounds were next assayed for effects on phosphorylated (p) Smad (p-Smad) 2/3 generation, and two of the four suppressed p-Smad2/3 formations (Figure 1C). Compound 2, napthoquinone, was previously reported to block renal cell EMT via inhibition of TGF-β1 signaling, although we did not observe inhibition of p-Smad2/3 (24). Nonetheless, we focused instead on the compound 4, methacycline, because of the clear inhibitory effect on TGF-β1–induced EMT by Western blot (Figure 1D), and the lack of direct effects on p-Smad2/3 formation in nontoxic concentrations (Figure 1E). Of note, we observed that methacycline consistently restored E-cadherin on cell borders by staining (Figure 1A), whereas the increase of total E-cadherin protein level was relatively incomplete and variable by comparison with control SB431542 (Figure 1D). Methacycline is a tetracycline antibiotic. Similar to other tetracyclines, it has been used extensively as an antimicrobial, due to inhibition of bacterial protein synthesis, but is not known to be active in tissue remodeling.

We next examined the effects of methacycline (5–10 μM) on sorted primary

alveolar epithelial cells (AECs) that are E-cadherin positive. We have previously reported that primary AECs undergo TGF-β1–dependent EMT when cultured on fibronectin-coated surface (25). This eventuates because AECs plated on the relatively stiff fibronectin surface robustly activate latent TGF-β1, which, in turn, induces expression of EMT proteins, collagen I, Snail1, and α-smooth muscle actin (α-SMA), and loss of cell border E-cadherin, whereas total E-cadherin levels don't change within 5 days. Methacycline attenuated TGF-β1–induced expression of the EMT proteins, collagen I, Snail1 (Figure 2A), and α-SMA (Figures 2A and 2B), as well as collagen I and Snail1 mRNA (Figure 2C), and restored cell border E-cadherin (Figure 2B), without affecting Smad2/3 phosphorylation for at least 5 days (Figure 2A). Of note, when we used the AECs without sorting, the contaminating fibroblasts (E-cadherin–negative cells) still expressed α-SMA in the presence of methacycline (*see* Figure E1 in the online supplement, and Figure 2B, *right panel*), even though α-SMA in epithelial cells was markedly suppressed. Consistent with this observation, the mesenchymal markers induced by TGF-β1 in primary lung fibroblasts detected by immunoblotting were not affected by methacycline, even at the concentration of 20 μM (Figure 2D), indicating that methacycline directly inhibits TGF-β1–induced expression of mesenchymal proteins in epithelial cells, but not in lung fibroblasts.

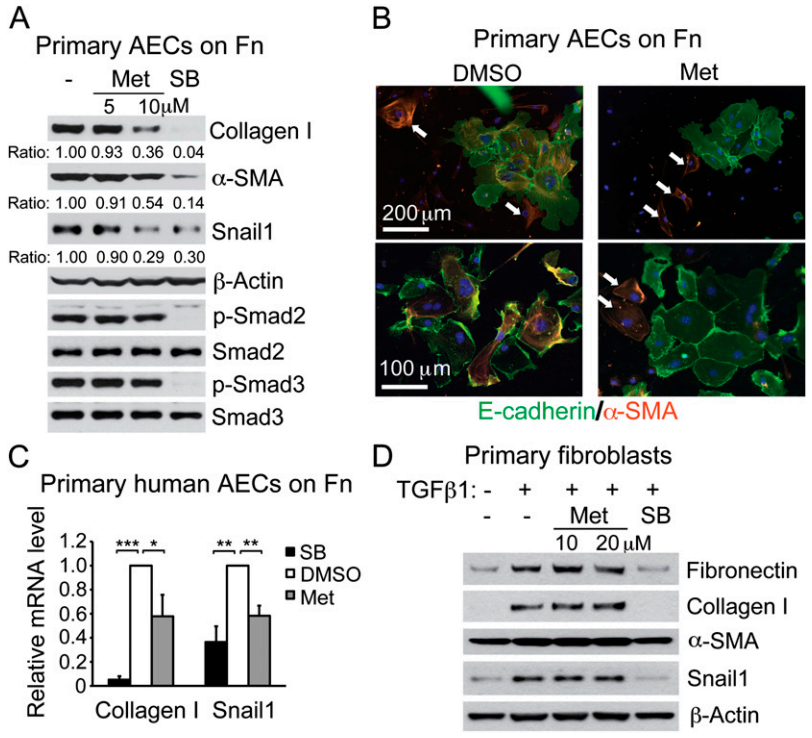

Figure 2. Met attenuates TGF-β1–dependent EMT in primary alveolar epithelial cells (AECs). Primary AECs were plated on fibronectin (Fn) for 5 days to allow latent TGF-β1 activation and the cells to undergo EMT. (*A*) Primary AECs on Fn were cultured in the presence of Met (5,10 μM) or SB (5 μM) and the lysates were blotted for collagen I, α-smooth muscle actin (α-SMA), Snail1, p-Smad2, total Smad2, p-Smad3, total Smad3, and β-actin. The relative intensity normalized to β-actin is shown. (*B*) Primary AECs on Fn incubated with Met (10 μM) or vehicle control DMSO were immunostained for E-cadherin (*green*) and α-SMA (*red*). Contaminating fibroblasts are indicated with *arrows*. (*C*) Primary human AECs on Fn were treated with DMSO, Met (10 μM), or SB (5 μM), and the mRNAs were assessed by quantitative RT-PCR (qRT-PCR) analysis. Collagen I and Snail1 mRNA levels are normalized to β-actin mRNA level. Data are expressed as relative fold change over DMSO (set at 1). Mean ± SEM of three independent experiments is shown, and Student's *t* test was performed (*$P < 0.05$, **$P < 0.01$, ***$P < 0.001$). (*D*) Primary fibroblasts were stimulated with TGF-β1 (4 ng/ml) and cultured in the presence of Met (10, 20 μM) or SB (5 μM) for 48 hours, and the lysates were blotted for Fn, collagen I, α-SMA, Snail1, and β-actin. (*A* and *D*) A representative blot of three independent experiments is shown.

Methacycline Inhibits Non-Smad, but Not Smad Signaling

To validate that methacycline does not directly block Smad signaling, we examined the influence of methacycline on TGF-β1–induced Smad transcriptional activity. A549 cells were transfected with either a 12× SBE–luciferase or a β-catenin/TCF (TOPFlash) reporter construct and then treated with TGF-β1 in the presence or absence of methacycline or SB431542. FOPFlash reporter, containing mutated TCF binding sites, was used as a negative control for TOPFlash. TGF-β1–stimulated SBE (Figure 3A) and TOPFlash (Figure 3B) activities at 48 hours were not significantly attenuated by methacycline, whereas both were completely abrogated by SB431542, consistent with results of p-Smad2/3 immunoblots (Figure 1E). We next asked whether the non-Smad TGF-β1 signaling pathway could be affected. In preliminary experiments, we found that TGF-β1 induced c-Jun N-terminal kinase (JNK), p38, extracellular signal–regulated kinase (ERK), and Akt activation in A549 cells within 15 minutes of stimulation. Methacycline blocked TGF-β1–induced JNK, p38, and Akt activation, but had no effect on ERK function (Figure 3C). Extending these data, we found that methacycline and specific inhibitors of JNK or p38 attenuated TGF-β1–induced mesenchymal markers, fibronectin and Snail1, in A549 cells, whereas specific ERK inhibitor had no effect (Figure 3D). Interestingly, JNK, p38, and ERK inhibitors had partial inhibitory effects on N-cadherin and vimentin expression, whereas methacycline had little effect on inhibition of these mesenchymal proteins. Both methacycline and p38 inhibitor suppressed α-SMA and Snail1 expression induced by TGF-β1 in AECs, whereas JNK inhibitor had partial effect on α-SMA expression, and ERK inhibitor had no effect (Figure 3E). In cultured primary fibroblasts there was constitutive activation of the above kinases in the absence of TGF-β1, and methacycline had no inhibitory effect (Figure E2). All these data imply that methacycline blocks TGF-β1–induced EMT at least in part through inhibiting TGF-β1–induced JNK, p38, and Akt activation. This conclusion is consistent

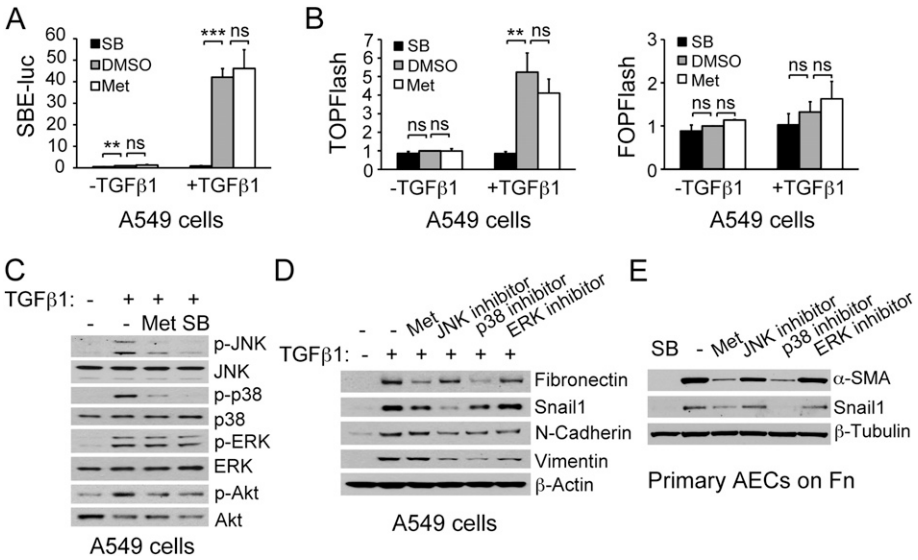

Figure 3. Met blocks TGF-β1–induced c-Jun N-terminal kinase (JNK), p38, and Akt activation, but not Smad-binding element (SBE) or TCF/β-catenin reporter activity. A549 cells expressing SBE-luciferase (luc) (*A*), TOPFlash, or FOPFlash (*B*) were serum starved overnight and then treated without or with TGF-β1 (4 ng/ml) in combination with DMSO, SB (5 μM), or Met (10 μM), and luc activity was determined after 24 hours. Relative activity was normalized to *Renilla* luc and relative fold change over DMSO without TGF-β1 (set at 1) was calculated. (*A* and *B*) Mean ± SEM of three independent experiments is shown, and Student's *t* test was performed. (***P* < 0.01, ****P* < 0.001; ns, not significant). (*C*) A549 cells serum-starved for 2 days were treated without or with TGF-β1 (4 ng/ml) in combination with DMSO (−), SB (5 μM), or Met (10 μM) for 15 minutes. Cell lysates were analyzed by immunoblotting with antibodies to p-JNK, JNK, p-p38, p38, extracellular signal–regulated kinase (ERK), p-ERK, p-Akt, and Akt. (*D*) A549 cells were treated without or with TGF-β1 (4 ng/ml) in combination with DMSO (−), Met (10 μM), JNK inhibitor (10 μM), p38 inhibitor (10 μM), or ERK inhibitor (10 μM) for 48 hours. Cell lysates were immunoblotted for Fn, Snail1, N-cadherin, vimentin, and β-actin. (*E*) Primary AECs on Fn were cultured in the presence of Met, JNK inhibitor, p38 inhibitor, or ERK inhibitor at 10 μM final concentration, and the lysates were blotted for α-SMA, Snail1, and β-tubulin. (*C–E*) A representative blot of three independent experiments is shown.

with prior studies showing that JNK, p38, and Akt activity regulates EMT responses to TGF-β1 stimulation (26). The lack of effect of methacycline on fibroblast JNK, p38, and Akt activities indicates that methacycline is likely not a direct kinase inhibitor.

Methacycline Improves Survival and Attenuates Fibrosis after Bleomycin-Induced Lung Injury

To explore a possible *in vivo* protective role of methacycline, adult female C57BL/6 mice were injected intratracheally with bleomycin in doses found to result in lethality in the majority of mice after 21 days (2.5 U/kg). To avoid possible effects of methacycline on the early injury and inflammatory phase after bleomycin, methacycline (100 mg/kg) was administered by intraperitoneal injection daily to 11 mice beginning after 10 days, during the fibrogenic phase. Control mice received vehicle alone. Treatment was repeated every day for 7 days. After this period, a significant increase in survival was observed in the methacycline-treated mice versus control mice (Figure 4A).

In parallel experiments, mice were given intratracheal bleomycin in a lower dose (2 U/kg) previously found to induce fibrosis in C57BL/6 mice, but to allow approximately 80% survival. Mice were again given daily methacycline beginning on Day 10 after bleomycin, and the lungs were harvested for analysis on Day 17. Levels of collagen I, fibronectin, and EMT transcription factors, Snail1 and Twist1, in extracts of injured lungs were assessed by immunoblotting, and the quantification of densitometry from each of three experiments was pooled for statistical analysis. Mice treated with bleomycin plus methacycline showed consistently decreased collagen I, fibronectin, Snail1, and Twist1 protein levels compared with mice given bleomycin but no drug (Figure 4B). Collagen I, fibronectin, and Twist1 mRNA levels in extracts of injured lungs were also significantly suppressed by methacycline treatment; however, Snail1 mRNA was neither induced by bleomycin nor affected by methacycline (Figure E3A), consistent with Snail1 regulation being post-transcriptional (27). Whole-lung collagen content was measured using Sircol assay, and fold changes compared with saline-treated mice from each of three experiments were pooled for statistical analysis. Bleomycin injury significantly increased collagen content in the lungs on Day 17, whereas bleomycin plus methacycline–treated mice had less collagen accumulation. The saline plus methacycline group showed no difference from the saline-only group (Figure 4C). Collagen I levels in BAL fluids were also dramatically up-regulated in bleomycin-injured mouse lungs, but decreased in bleomycin plus methacycline–treated mice. There was essentially no detectable BAL collagen I in saline-treated mice (Figure 4D).

Fibrogenesis was also examined by trichrome staining and immunostaining. Quantification of trichrome staining, expressed as percent lung area showing trichrome blue staining, revealed attenuated collagen accumulation in lungs of bleomycin plus methacycline–treated mice (Figure E3B), consistent with the biochemical assays and improved survival. Sections of lungs from mice treated with saline, bleomycin, or bleomycin plus methacycline were immunostained for E-cadherin and α-SMA. Accumulation of α-SMA was attenuated in lungs of mice given methacycline (Figure 4E). Overall, these findings indicate that methacycline administered *in vivo* attenuates bleomycin-induced fibrogenesis.

We next asked whether JNK, p38, or Akt activities were affected *in vivo* on Day 17 by the 7-day methacycline treatment. However, p-JNK, p-p38, or p-Akt levels showed no difference between the bleomycin and bleomycin plus methacycline groups on Day 17 in immunoblots, due to high levels of these proteins in macrophages. We then attempted to focus on epithelial cell–specific p-JNK, p-p38, and p-Akt by immunostaining, but again, we could not discern clear differences. One possible reason could be that it was too late to examine early signaling effects on Day 17, when transcriptional regulation of collagen I, fibronectin, and Twist1 had already occurred.

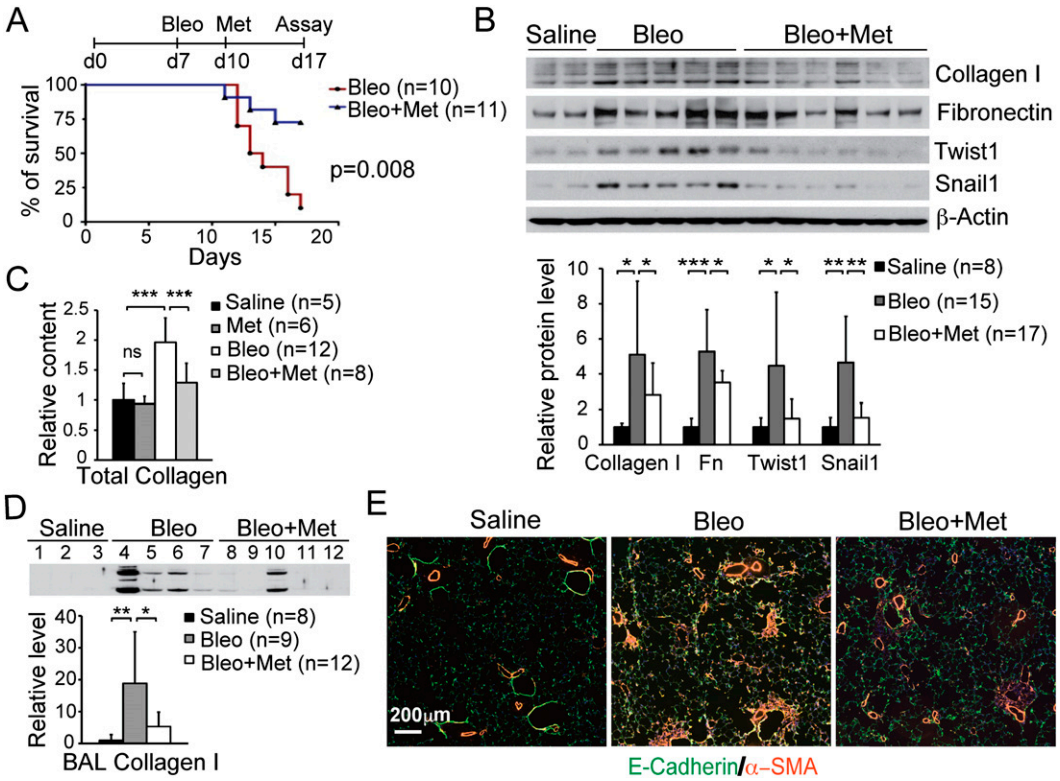

Figure 4. Met attenuates TGF-β1–stimulated EMT and bleomycin (Bleo)-induced fibrogenesis. (*A*) Mice were injected intratracheally with Bleo (2.5 U/kg). After 10 days, Met 100 mg/kg or vehicle alone was administered intraperitoneally daily for 7 days. The survival of Bleo-treated mice by Day 17 was plotted and analyzed. (*B*) EMT markers measured in protein extracts from snap-frozen mouse lungs treated with saline, Bleo, or Bleo + Met. Tissue lysates were blotted for collagen I, Fn, Twist1, Snail1, and β-actin (*upper panel*). Densitometry values of collagen I, Fn, Twist1, and Snail1 blots were normalized to that of β-actin, and the normalized values of saline were set at 1. Quantification (mean ± SEM) of EMT markers from three independent experiments (total of 8 mice given saline, 15 given Bleo, and 17 given Bleo + Met) is shown in the *lower panel*. (*C*) Total lung collagen levels measured by Sircol assay. Pepsin- and acid-soluble collagen content from mice treated with saline + Met, Bleo, and Bleo + Met was normalized to that of saline-treated lungs. Mean ± SEM of the fold changes from three independent experiments was quantified. (*D*) Collagen I level measured in bronchoalveolar lavage (BAL) fluid by immunoblots. BAL supernatant (50 μl) from mice treated with saline, Bleo, and Bleo + Met was blotted for collagen I (*upper panel*). Quantification (mean ± SEM) of the densitometry values of collagen I from three independent experiments is shown in the *lower panel*. (*E*) Low-power section of 17-day Bleo-injured lung without or with 7-day Met immunostained with E-cadherin (*green*) and α-SMA (*red*). Saline-treated lung section was used as staining control. *Scale bar*, 200 μm. (*B* and *D*) A representative blot of three independent experiments is shown. (*B–D*) $^*P < 0.05$, $^{**}P < 0.01$, $^{***}P < 0.001$; ns, not significant by *t* test.

Of interest, we observed that methacycline treatment significantly decreased p-Smad2/3 levels in the lung lysates on Day 17 after bleomycin (Figure E3C), whereas it did not affect p-Smad2/3 levels in saline control mice (Figure E3D), implying that methacycline affects Smad signaling indirectly through regulation of non-Smad signaling, likely through TGF-β1 itself and TGF-β receptor levels (Figure E3C), which then further attenuates EMT and fibrosis *in vivo*.

Inflammation and Macrophage TGF-β1 Signaling Are Not Affected by Methacycline

Although methacycline attenuates bleomycin-induced fibrogenesis and inhibits EMT *ex vivo* and *in vivo*, it is not necessarily the case that methacycline works *in vivo* via inhibition of EMT directly. It is possible that macrophages, known to contribute to fibrogenesis, are directly targeted by methacycline. To examine this, BAL fluids were collected from mice injected with saline or bleomycin with or without methacycline treatment. Total protein (Figure 5A) was attenuated in bleomycin-injected mice treated with methacycline. In contrast, total BAL cell counts (Figure 5B) and immune cell percentage in the BAL (Figure 5C) were not affected, suggesting that methacycline does not suppress inflammation. Methacycline did decrease p-Smad2 level in macrophages on Day 17 (Figure 5D); however, TGF-β1–responsive genes (osteopontin, metalloproteinase [MMP]-19, plasminogen activator inhibitor type 1 [PAI1], and triggering receptor expressed on myeloid cells [TREM]-1) in BAL macrophages were not changed by methacycline (Figure 5E), indicating that the observed decrease in p-Smad2 levels was insufficient to discernibly modify TGF-β1 target genes in macrophages.

Doxycycline, but Not Tetracycline, also Blocks EMT

Methacycline is a tetracycline antibiotic. None of eight other tetracyclines tested in our screen was identified as having significant EMT-inhibitory activity originally. However, doxycycline, although

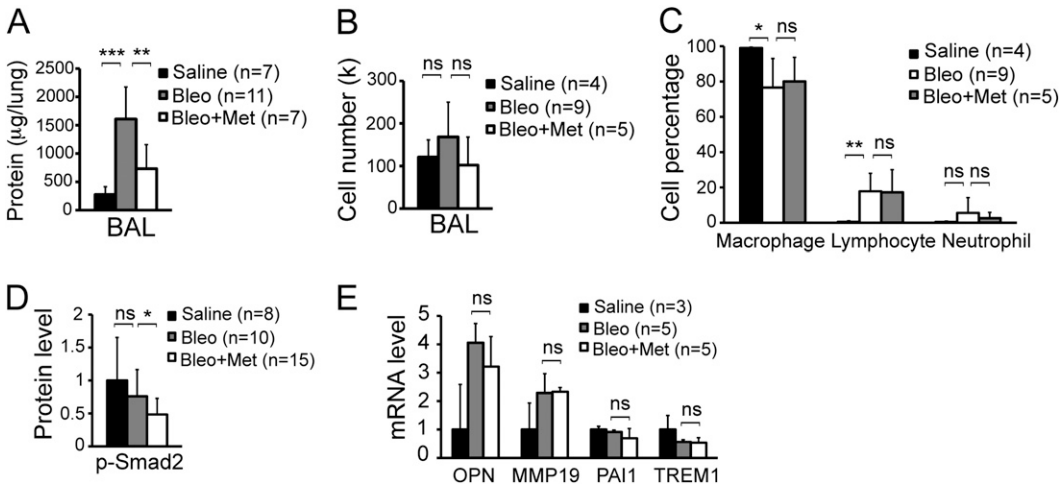

Figure 5. Fibrogenic response in mouse BAL fluid. (*A*) Total protein concentration (μg/lung) from BAL 17 days after intratracheal saline (n = 7), Bleo (n = 11), or Bleo + Met (n = 7). Cell counts (*B*) and immune cell distribution (*C*) from BAL of mice intratracheally injected with saline (n = 4), Bleo (n = 9), or Bleo + Met (n = 5). (*D*) Quantification (mean ± SEM) of p-Smad2 protein from three independent experiments (total of 8 mice given saline, 10 given Bleo, and 15 given Bleo + Met) analyzed by immunoblotting BAL cell pellets. Data are expressed as relative fold change over saline values (set at 1). (*E*) Transcripts of TGF-β1–responsive genes were measured in RNA extracts from BAL pellets treated with saline (n = 3), Bleo (n = 5), or Bleo + Met (n = 5) by qRT-PCR analysis. Osteopontin (OPN), metalloproteinase (MMP)-19, plasminogen activator type I (PAI)-1, and TREM1 mRNA levels are normalized to β-actin mRNA level. (*A–E*) $^*P < 0.05$, $^{**}P < 0.01$, $^{***}P < 0.001$; ns, not significant by t test.

showing only weak activity (~20% inhibition on fibronectin induction) in our 5-μM EMT screen, has recently been reported to attenuate bleomycin-induced pulmonary fibrosis (28, 29), prompting us to further examine this compound and another inactive analog, tetracycline (Figure 6A). Indeed, we observed that doxycycline and methacycline have similar activity in blocking TGF-β1–induced EMT in A549 cells, as revealed by decrease of fibronectin and Snail1, and neither of them inhibited N-cadherin and vimentin (Figure 6B). Tetracycline did not have any effect. Likewise, in primary AECs, doxycycline, but not tetracycline, decreased α-SMA and Snail1 by immunoblotting (Figure 6C), and attenuated TGF-β1–induced α-SMA and increased cell border E-cadherin by immunostaining (Figure 6D). Doxycycline and methacycline, but not tetracycline, also inhibited TGF-β1–dependent α-SMA in immortalized AECs by immunostaining (Figure E4A) and immunoblotting (Figure E4B). Taken together, doxycycline and methacycline appear to have similar inhibitory effects on TGF-β1–induced EMT in both A549 cells and lung epithelial cells, although doxycycline is not as potent as methacycline.

The family of tetracyclines is reported to inhibit MMP activity through chelation of the zinc ion at the active site of the enzyme (30). The ability of doxycycline to attenuate fibrosis was thought to be due to inhibition of MMP activity (29, 31). In our system, MMP inhibitor, GM6001, had no effect on TGF-β1–induced EMT (Figures 6C–6E), indicating that methacycline and doxycyline inhibit EMT through a different mechanism than MMP inhibition.

Discussion

The series of experiments reported here indicate that a phenotypic screen based specifically on inhibition of AEC EMT *in vitro* can identify tool compounds that attenuate lung fibrogenesis *in vivo*. Moreover, the novel compound reported here, methacycline, blocks EMT *in vitro* and fibrogenesis *in vivo* without directly affecting TGF-β1 Smad signaling. Instead, methacycline appears to act, at least in part, through inhibition of several non-Smad pathways activated via TGF-β1: p38, JNK, and Akt. In addition, the inhibitory effect on non-Smad signaling was only observed in epithelial cells, but not in fibroblasts, indicating that methacycline is not a direct kinase inhibitor. Exactly how this pattern of inhibition is achieved is unclear, but the inhibitory effects of methacycline on several non-Smad pathways imply that methacycline is acting very proximally in TGF-β1 signaling. The observed protective effects of inhibition of the non-Smad arm of TGF-β1 signaling is consistent with prior reports that Jun kinase, phosphoinositide 3-kinase (PI3K)/Akt, and p38 activities are each required for damaging fibrogenesis after bleomycin-induced lung injury (20, 32, 33). In addition, consistent with our observations, mice deficient in Jun kinase show suppression of fibrosis, but not inflammation after bleomycin-induced injury (32). It remains to be defined whether additional signaling pathways not studied in our experiments are also important to the inhibitory effects of methacycline *in vivo*. This is possible, because the pattern of inhibition of mesenchymal proteins in TGF-β1–stimulated epithelial cells by specific inhibitors of JNK or p38 kinase did not completely match the inhibitory effects of methacycline (Figure 3). Nonetheless, these studies with methacycline support the paradigm that activation of the non-Smad TGF-β1–dependent pathways act to promote, and actually determine, the epithelial and tissue responses to Smad signaling both *in vitro* and *in vivo* (34, 35).

Although methacycline's inhibitory effects on TGF-β1–induced expression of mesenchymal proteins is restricted to epithelial cells *in vitro*, we recognize that this is not necessarily the case *in vivo*. The data show that numerous markers of mesenchymal expansion, including the

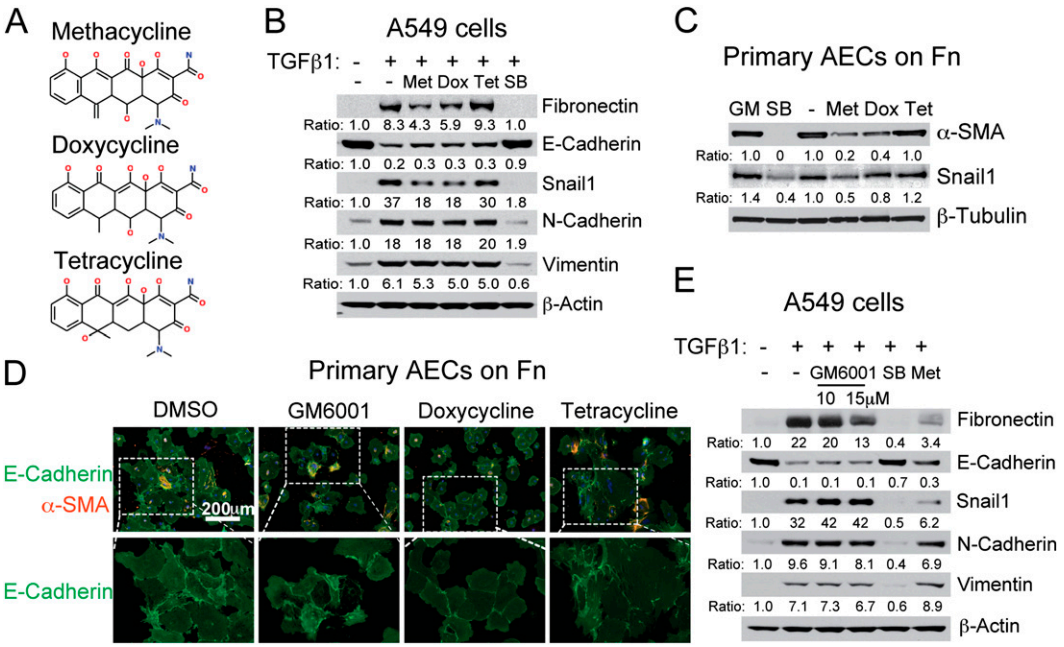

Figure 6. Doxyclycline (Dox) inhibits TGF-β1–induced EMT in A549 and lung epithelial cells. (*A*) Two-dimensional structures of Met, Dox, and tetracycline (Tet). (*B*) A549 cells were treated without or with TGF-β1 (4 ng/ml) in combination with DMSO (−), Met (10 μM), Dox (10 μM), Tet (10 μM), or SB (5 μM) for 48 hours. Cell lysates were immunoblotted for Fn, E-cadherin, Snail1, N-cadherin, vimentin, and β-actin. (*C*) Primary AECs on Fn were cultured in the presence of GM6001 (GM) (10 μM), SB (5 μM), DMSO (−), Met (10 μM), Dox (10 μM), or Tet (10 μM), and the lysates were blotted for α-SMA, Snail1, and β-tubulin. (*D*) Primary AECs on Fn incubated with DMSO, GM (10 μM), Dox (10 μM), or Tet (10 μM) were immunostained for E-cadherin (*green*) and α-SMA (*red*). *Scale bar*, 200 μm. (*E*) A549 cells were treated without or with TGF-β1 (4 ng/ml) in combination with DMSO (−), GM (10 μM), SB (5 μM), or Met (10 μM) for 48 hours. Cell lysates were immunoblotted for Fn, E-cadherin, Snail1, N-cadherin, vimentin, and β-actin. (*B*, *C*, and *E*) A representative blot of three independent experiments is shown. The relative intensity normalized to β-actin is labeled.

important transcription factor, Snail1, and several mesenchymal proteins known to be downstream of Snail signaling, including collagen I and fibronectin, are all suppressed in whole-lung lysates by methacycline. Indeed, five different assays of collagen expression after bleomycin-induced lung injury all consistently showed that at least 50% of the increase in collagen during the fibrogenic phase was blocked by methacycline (Figures 4B–4D, and Figures E3A and E3B). Because the bulk of collagen likely comes from expansion of resident mesenchymal cells, and activation of Snail1 in mesenchymal cells is known to promote mesenchymal expansion (27), it seems likely that mesenchymal cell Snail1 and Twist1 expression is also suppressed by methacycline *in vivo*, even though we could not measure direct effects of methacycline on lung fibroblast Snail1 *in vitro*. An appealing possibility is that abrogation of EMT attenuates epithelial-derived signals, including active TGF-β1 itself, that act to induce mesenchymal cell Snail1 and other drivers of mesenchymal expansion. Other secondary effects of methacycline not immediately due to direct effects on TGF-β1–induced non-Smad activation are also apparent. For example, whole-lung p-Smad2 and p-Smad3 levels are lower than untreated controls on Day 17 after bleomycin (Figure E3C). The level of both of these proteins is suppressed on Day 17, and yet we can find no evidence that methacycline directly affects p-Smad2/3 formation (Figures 1E and 2A and Figure E5) or signaling (SBE reporter activity; Figure 3A) within 24 hours. We favor the view that attenuation of epithelial EMT signaling promoting a fibrotic process leads to secondary suppression of numerous mediators of an active fibrotic process, including whole-lung Snail1, TGF-β receptor II (Figure E3C), and p-Smad2/3 levels, which further attenuate fibrogenesis. This could also be true in epithelial cells that long incubations (over 24 h) with methacycline induce a secondary inhibition on p-Smad2/3 and TGF-β receptor II (Figure E5), possibly through feedback effects of abrogated non-Smad signaling.

Inhibitors of a number of signaling pathways important for EMT have been reported to block fibrosis *in vivo*. The most extensively tested and consistent inhibitors are those that block accumulation of p-Smads: inhibition of latent TGF-β1 activation, TGF-β1 receptor kinase activity, or Smad3 deficiency. More recently, inhibitors of EMT that target interactions between Smad and β-catenin signaling have been reported to attenuate fibrosis *in vivo* (17). A number of other inhibitors of EMT *in vitro* have been identified, but their effects on fibrogenesis are unknown (36–38). Recently, inhibition of Akt was shown to suppress EMT and fibrosis *in vivo* in mice deficient in epithelial phosphatase and tensin homolog (PTEN), which display enhanced epithelial PI3K and Akt activities (20). Methacycline appears to act by a mechanism distinct from prior EMT inhibitors with *in vivo* activity, raising the possibility that this point of inhibition could provide some therapeutic synergy with other effective inhibitors of fibrogenesis.

Although our identification of methacycline as a novel suppressor of fibrosis came from an unbiased screen

of a small-molecule library, an active analog of methacycline, doxycycline (Figure 6A), has shown activity in several prior studies of fibrosis, including bleomycin-induced pulmonary fibrosis in mice, as well as models of fibrosis in other tissues (28, 39). Fujita and colleagues (29) described attenuation of bleomycin-induced lung fibrosis by doxycycline when administered orally from Days 14 to 28 after bleomycin. Collagen accumulation, but not inflammation, was suppressed by doxycycline, and the effects ascribed to epithelial cells, but not fibroblasts. Like most other studies of doxycycline, and many tetracyclines, the mechanism of inhibition was thought to be due its activity as an MMP inhibitor (29, 31). All tetracyclines feature an enol backbone that has divalent cation binding activity responsible for the reported MMP inhibition found in several members of this class (30). However, recent studies of MMP 9 inhibition by doxycycline *in vitro* show the effective dose range to be 50–100 μM (31). Methacycline and doxycycline were effective in our *in vitro* EMT assays at 5–10 μM, and inhibition of MMPs with a broad spectrum inhibitor (GM6001) did not abrogate EMT in these assays (Figures 6C–6E). Moreover, MMP9-deficient mice are not protected from bleomycin-induced lung fibrosis (40). Prior observations that BAL MMP activity is reduced in mice and patients with IPF given doxycycline could represent secondary suppression of MMPs from attenuation of fibrogenesis through pathways elucidated here with methacycline (28, 31). For example, p-Smad2/3 levels in whole lungs are clearly lower after methacycline delivery for 7 days, even though the compound does not directly affect Smad signaling (Figures 1E, 2A, and 3A and Figure E3C). In this context, lower MMP activity in BAL fluids from patients with IPF given doxycycline could be a biomarker for drug activity rather than an important drug target. Overall, the studies with methacycline reported here provide a different prism for interpreting prior studies of doxycycline, and support the concept of further clinical studies of this class of drugs in attenuating progression of fibrotic disease. ■

Author disclosures are available with the text of this article at www.atsjournals.org.

Acknowledgments: The authors appreciate the technical assistance of Irene Kwan, Victor Tan, and Irina Krylova.

References

1. Maitra M, Wang Y, Gerard RD, Mendelson CR, Garcia CK. Surfactant protein A2 mutations associated with pulmonary fibrosis lead to protein instability and endoplasmic reticulum stress. *J Biol Chem* 2010;285:22103–22113.
2. Kuwano K, Kunitake R, Kawasaki M, Nomoto Y, Hagimoto N, Nakanishi Y, Hara N. P21Waf1/Cip1/Sdi1 and p53 expression in association with DNA strand breaks in idiopathic pulmonary fibrosis. *Am J Respir Crit Care Med* 1996;154:477–483.
3. Korfei M, Ruppert C, Mahavadi P, Henneke I, Markart P, Koch M, Lang G, Fink L, Bohle RM, Seeger W, *et al*. Epithelial endoplasmic reticulum stress and apoptosis in sporadic idiopathic pulmonary fibrosis. *Am J Respir Crit Care Med* 2008;178:838–846.
4. Tanjore H, Blackwell TS, Lawson WE. Emerging evidence for endoplasmic reticulum stress in the pathogenesis of idiopathic pulmonary fibrosis. *Am J Physiol Lung Cell Mol Physiol* 2012;302: L721–L729.
5. Lawson WE, Cheng DS, Degryse AL, Tanjore H, Polosukhin VV, Xu XC, Newcomb DC, Jones BR, Roldan J, Lane KB, *et al*. Endoplasmic reticulum stress enhances fibrotic remodeling in the lungs. *Proc Natl Acad Sci USA* 2011;108:10562–10567.
6. Zhong Q, Zhou B, Ann DK, Minoo P, Liu Y, Banfalvi A, Krishnaveni MS, Dubourd M, Demaio L, Willis BC, *et al*. Role of endoplasmic reticulum stress in epithelial–mesenchymal transition of alveolar epithelial cells: effects of misfolded surfactant protein. *Am J Respir Cell Mol Biol* 2011;45:498–509.
7. Selman M, Pardo A. Role of epithelial cells in idiopathic pulmonary fibrosis: from innocent targets to serial killers. *Proc Am Thorac Soc* 2006;3:364–372.
8. Chapman HA. Epithelial responses to lung injury: role of the extracellular matrix. *Proc Am Thorac Soc* 2012;9:89–95.
9. Crosby LM, Waters CM. Epithelial repair mechanisms in the lung. *Am J Physiol Lung Cell Mol Physiol* 2010;298:L715–L731.
10. Pan LH, Yamauchi K, Uzuki M, Nakanishi T, Takigawa M, Inoue H, Sawai T. Type II alveolar epithelial cells and interstitial fibroblasts express connective tissue growth factor in IPF. *Eur Respir J* 2001;17: 1220–1227.
11. Moore BB, Coffey MJ, Christensen P, Sitterding S, Ngan R, Wilke CA, McDonald R, Phare SM, Peters-Golden M, Paine R , III, *et al*. GM-CSF regulates bleomycin-induced pulmonary fibrosis via a prostaglandin-dependent mechanism. *J Immunol* 2000;165: 4032–4039.
12. Horan GS, Wood S, Ona V, Li DJ, Lukashev ME, Weinreb PH, Simon KJ, Hahm K, Allaire NE, Rinaldi NJ, *et al*. Partial inhibition of integrin αvβ6 prevents pulmonary fibrosis without exacerbating inflammation. *Am J Respir Crit Care Med* 2008;177:56–65.
13. Munger JS, Huang X, Kawakatsu H, Griffiths MJ, Dalton SL, Wu J, Pittet JF, Kaminski N, Garat C, Matthay MA, *et al*. The integrin alpha v beta 6 binds and activates latent TGF beta 1: a mechanism for regulating pulmonary inflammation and fibrosis. *Cell* 1999;96: 319–328.
14. Thiery JP, Acloque H, Huang RY, Nieto MA. Epithelial–mesenchymal transitions in development and disease. *Cell* 2009;139:871–890.
15. Willis BC, Liebler JM, Luby-Phelps K, Nicholson AG, Crandall ED, du Bois RM, Borok Z. Induction of epithelial–mesenchymal transition in alveolar epithelial cells by transforming growth factor-beta1: potential role in idiopathic pulmonary fibrosis. *Am J Pathol* 2005;166: 1321–1332.
16. Vaughan AE, Chapman HA. Regenerative activity of the lung after epithelial injury. *Biochim Biophys Acta* 2013;1832:922–930.
17. Henderson WR Jr, Chi EY, Ye X, Nguyen C, Tien YT, Zhou B, Borok Z, Knight DA, Kahn M. Inhibition of Wnt/beta-catenin/CREB binding protein (CBP) signaling reverses pulmonary fibrosis. *Proc Natl Acad Sci USA* 2010;107:14309–14314.
18. Kim KK, Wei Y, Szekeres C, Kugler MC, Wolters PJ, Hill ML, Frank JA, Brumwell AN, Wheeler SE, Kreidberg JA, *et al*. Epithelial cell alpha3beta1 integrin links beta-catenin and Smad signaling to promote myofibroblast formation and pulmonary fibrosis. *J Clin Invest* 2009;119:213–224.
19. Kim Y, Kugler MC, Wei Y, Kim KK, Li X, Brumwell AN, Chapman HA. Integrin alpha3beta1–dependent beta-catenin phosphorylation links epithelial Smad signaling to cell contacts. *J Cell Biol* 2009;184: 309–322.
20. Miyoshi K, Yanagi S, Kawahara K, Nishio M, Tsubouchi H, Imazu Y, Koshida R, Matsumoto N, Taguchi A, Yamashita S, *et al*. Epithelial Pten controls acute lung injury and fibrosis by regulating alveolar epithelial cell integrity. *Am J Respir Crit Care Med* 2013;187: 262–275.
21. Tanjore H, Cheng DS, Degryse AL, Zoz DF, Abdolrasulnia R, Lawson WE, Blackwell TS. Alveolar epithelial cells undergo epithelial-to-mesenchymal transition in response to endoplasmic reticulum stress. *J Biol Chem* 2011;286:30972–30980.
22. Ulsamer A, Wei Y, Kim KK, Tan K, Wheeler S, Xi Y, Thies RS, Chapman HA. Axin pathway activity regulates *in vivo* pY654-β-catenin accumulation and pulmonary fibrosis. *J Biol Chem* 2012;287: 5164–5172.

23. Rowe RG, Lin Y, Shimizu-Hirota R, Hanada S, Neilson EG, Greenson JK, Weiss SJ. Hepatocyte-derived Snail1 propagates liver fibrosis progression. *Mol Cell Biol* 2011;31:2392–2403.
24. Reese S, Vidyasagar A, Jacobson L, Acun Z, Esnault S, Hullett D, Malter JS, Djamali A. The Pin 1 inhibitor juglone attenuates kidney fibrogenesis via Pin 1–independent mechanisms in the unilateral ureteral occlusion model. *Fibrogenesis Tissue Repair* 2010;3:1.
25. Kim KK, Kugler MC, Wolters PJ, Robillard L, Galvez MG, Brumwell AN, Sheppard D, Chapman HA. Alveolar epithelial cell mesenchymal transition develops *in vivo* during pulmonary fibrosis and is regulated by the extracellular matrix. *Proc Natl Acad Sci USA* 2006;103: 13180–13185.
26. Alcorn JF, Guala AS, van der Velden J, McElhinney B, Irvin CG, Davis RJ, Janssen-Heininger YM. Jun N-terminal kinase 1 regulates epithelial-to-mesenchymal transition induced by TGF-beta1. *J Cell Sci* 2008;121:1036–1045.
27. Rowe RG, Li XY, Hu Y, Saunders TL, Virtanen I, Garcia de Herreros A, Becker KF, Ingvarsen S, Engelholm LH, Bommer GT, *et al*. Mesenchymal cells reactivate Snail1 expression to drive three-dimensional invasion programs. *J Cell Biol* 2009;184:399–408.
28. Fujita M, Ye Q, Ouchi H, Harada E, Inoshima I, Kuwano K, Nakanishi Y. Doxycycline attenuated pulmonary fibrosis induced by bleomycin in mice. *Antimicrob Agents Chemother* 2006;50:739–743.
29. Fujita H, Sakamoto N, Ishimatsu Y, Kakugawa T, Hara S, Hara A, Amenomori M, Ishimoto H, Nagata T, Mukae H, *et al*. Effects of doxycycline on production of growth factors and matrix metalloproteinases in pulmonary fibrosis. *Respiration* 2011;81: 420–430.
30. Castro MM, Kandasamy AD, Youssef N, Schulz R. Matrix metalloproteinase inhibitor properties of tetracyclines: therapeutic potential in cardiovascular diseases. *Pharmacol Res* 2011;64: 551–560.
31. Mishra A, Bhattacharya P, Paul S, Paul R, Swarnakar S. An alternative therapy for idiopathic pulmonary fibrosis by doxycycline through matrix metalloproteinase inhibition. *Lung India* 2011;28:174–179.
32. Alcorn JF, van der Velden J, Brown AL, McElhinney B, Irvin CG, Janssen-Heininger YM. c-Jun N-terminal kinase 1 is required for the development of pulmonary fibrosis. *Am J Respir Cell Mol Biol* 2009; 40:422–432.
33. Matsuoka H, Arai T, Mori M, Goya S, Kida H, Morishita H, Fujiwara H, Tachibana I, Osaki T, Hayashi S. A p38 MAPK inhibitor, FR-167653, ameliorates murine bleomycin–induced pulmonary fibrosis. *Am J Physiol Lung Cell Mol Physiol* 2002;283:L103–L112.
34. Guo X, Wang XF. Signaling cross-talk between TGF-beta/BMP and other pathways. *Cell Res* 2009;19:71–88.
35. Xu P, Liu J, Derynck R. Post-translational regulation of TGF-β receptor and Smad signaling. *FEBS Lett* 2012;586:1871–1884.
36. Fang LP, Lin Q, Tang CS, Liu XM. Hydrogen sulfide attenuates epithelial–mesenchymal transition of human alveolar epithelial cells. *Pharmacol Res* 2010;61:298–305.
37. Felton VM, Borok Z, Willis BC. N-acetylcysteine inhibits alveolar epithelial–mesenchymal transition. *Am J Physiol Lung Cell Mol Physiol* 2009;297:L805–L812.
38. Zhou B, Buckley ST, Patel V, Liu Y, Luo J, Krishnaveni MS, Ivan M, DeMaio L, Kim KJ, Ehrhardt C, *et al*. Troglitazone attenuates TGF-β1–induced EMT in alveolar epithelial cells via a PPARγ-independent mechanism. *PLoS ONE* 2012;7:e38827.
39. Hori Y, Kunihiro S, Sato S, Yoshioka K, Hara Y, Kanai K, Hoshi F, Itoh N, Higuchi S. Doxycycline attenuates isoproterenol-induced myocardial fibrosis and matrix metalloproteinase activity in rats. *Biol Pharm Bull* 2009;32:1678–1682.
40. Betsuyaku T, Fukuda Y, Parks WC, Shipley JM, Senior RM. Gelatinase B is required for alveolar bronchiolization after intratracheal bleomycin. *Am J Pathol* 2000;157:525–535.